The Journal of the Oceanological Society of Korea
Vol. 22, No. 2, p. 63-70, June 1987.

A Summer Circulation Inferred from the Density (Temperature) Distribution in the Eastern Yellow Sea

Young-Ho Seung
Department of Oceanography, Inha University, Incheon 160, Korea

密度(水温) 分布에 의한 夏季黃海東部의 海水循環考察

承 永 鎬
仁荷大 海洋學科

Abstract

Existing oceanographic data indicate that tidal mixing fronts generally prevail in the Eastern Yellow Sea along the Korean coast. In the Western part, these fronts seem to be much weaker. These fronts are believed to be generated mostly by spatially different tidal mixing. The geostrophic adjustment model applied to the observed density structure gives the mixed coastal water flowing northward and the offshore waters (both surface warm and bottom cold waters) flowing southward along the Korean coast. The transport of each water amounts to $O(10^4)m^3/sec$.

요약 : 기존 해양조사 자료에 의하면 황해 동부는 일반적으로 한국연안을 따라 형성되는 조석전선으로 특징지어진다. 황해서부에서는 이러한 조석전선이 약하게 나타나는 듯하다. 이러한 현상은 장소에 따라 그 강도가 다른 조석혼합에 기인된다 하겠다. 추정된 밀도구조에 기존 地衡調整 모델을 적용한 결과 연안의 혼합수는 북향, 외양의 성층수(표층 및 저층)는 남향함이 밝혀졌다. 이들 각 수괴의 수송량은 약 $10^4 m^3/sec$로 나타났다.

INTRODUCTION

The Yellow Sea is generally very shallow (less than 100 m) with deepest part occuring in central area. It is characterized by strong tidal motion throughout the year and by intense surface cooling in winter. As summarized by Lie (1984), a cold water mass called the Yellow Sea Bottom Cold Water (hereafter YSBCW) occupies the bottom layer of the deepest part. This water is formed in winter by intense cooling. Temperature structure in winter is such that water columns are vertically homogeneous due to strong convective mixing and wind stirring.

In summer, the surface water is heated from above by solar radiation. The absorbed heat cannot generally penetrate into the deep layer, resulting in a strong thermocline which seperates the YSBCW from the surface warm water. However, the strong tidal action over the shallow coastal area may reduce much this stratification by vertical mixing. An evidence of strong tidal mixing over the coastal area can be provided by Choi's (1980, Fig. 12) tidal numerical experiment in which there is a contrast in tidal energy dissipation between coastal and offshore areas in the Eastern Yellow Sea. The resulting temperature structure may be such that, in the vertical section perpendicular to the coastline, the offshore water is warmer at the surface whereas colder at the bottom than the coastal water, resulting in the surface and bottom fronts. Though

there may be some localities due to the fresh water input by river discharge (cf., KORDI, 1986), the thermal front running along the coastline seem to be the general feature of the basin, especially in the eastern part (cf., Fig. 1). This fact will be discussed more later in this paper.

The main purpose of this paper is to estimate the mean circulation of the Eastern Yellow Sea based on the assumption that the geostrophic adjustment model can be applied to the observed density structure in this area.

TEMPERATURE AND DENSITY STRUCTURE

The vertical temperature and density sections obtained along the coast in the eastern part of the Yellow Sea (Fig. 2a and b, and Fig. 3a through e) are generally characterized by tidally mixed coastal water and stratified offshore water. The salinity distributions are improper to observe the frontal structures and do not show the same character because the salinity does not reflect the solar heating at the surface which is the major factor determining

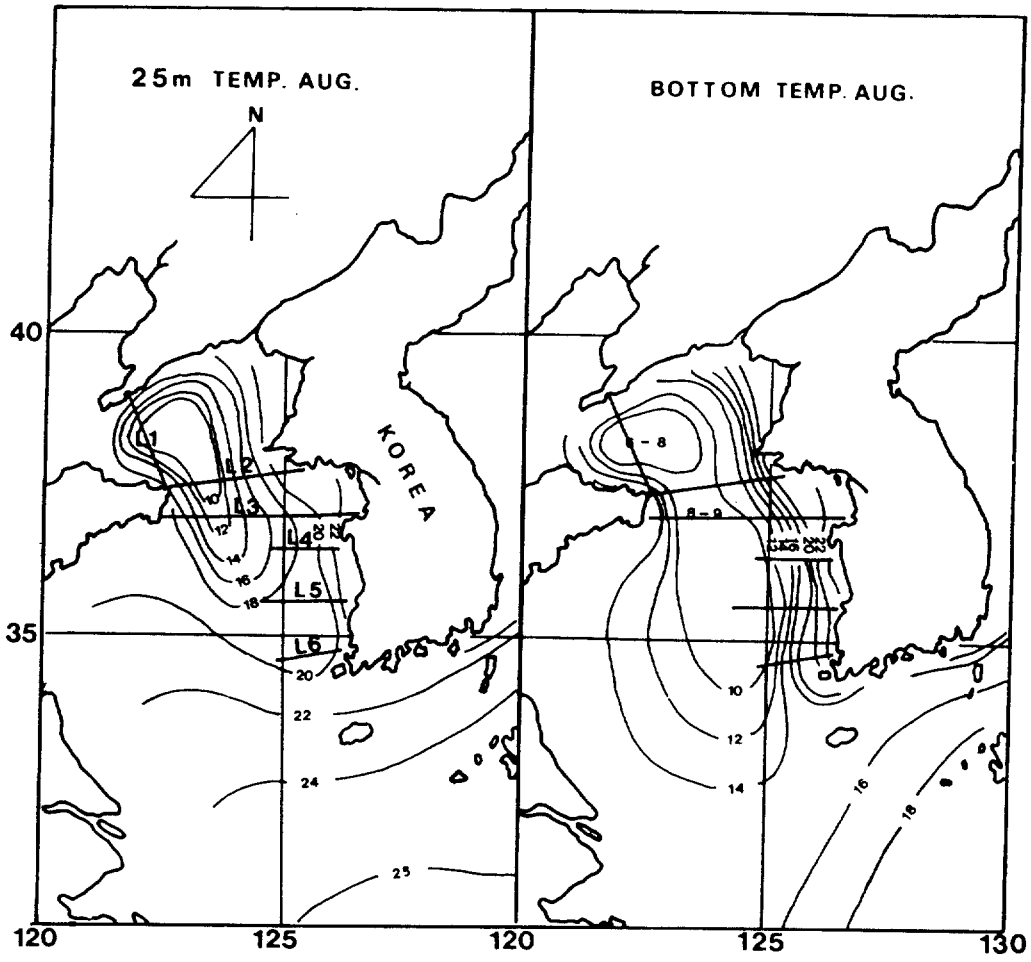

Fig. 1. Horizontal temperature distribution at 25m depth and the bottom in August in the Yellow Sea. Numbers on isolines are in degree centigrade. Lines marked by L1 through L6 are density (temperature) sections shown in Fig. 2 and 3. Data are from Fisheries Experiment Station and averaged over 1921-1945.

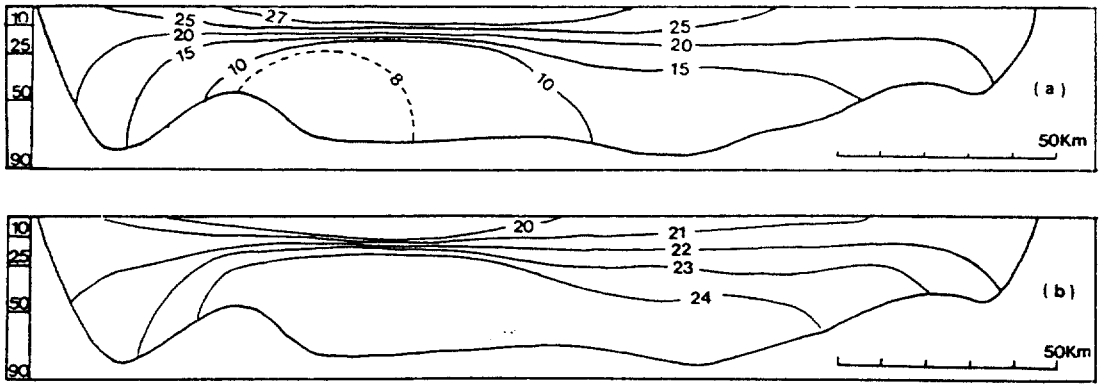

Fig. 2. a) Temperature and b) density structures on the section L2 (see Fig. 1 for location) obtained in August, 1939 by Fisheries Experiment Station. Right (left) end is the eastern (western) coast. Depths are in meters and temperatures (densities) are in degree centigrade (sigma-t) on isolines.

the stratification of the offshore water. In fact, most salt sinks are located along the lateral boundaries (fresh water discharge by rivers) and they are not believed to affect the vertical structures of density unless intense evaporation occurs. In reality, the salinity variation in this region is not generally large enough to control the density structure so that there is a good similarity between the temperature and density structures as shown by Fig. 2a and b as an example. Though not observed in Fig. 2 and 3, much smaller scale salinity-induced density fronts may occur in the vicinity of river mouths. However, we consider here only the basin-scale circulation so that the smaller scale motions arisen from the small localities, such as the fresh water discharge in the vicinity of river mouths, can be neglected. Though the frontal structure is relatively weak in section L1 (Fig. 3a), and density sections L4 through L6 (Fig. 3c through e, respectively) do not cross the basin completely, it may be learned from all these figures (sections L1 through L6 in Fig. 2 and 3) that the tidal mixing effects extend up to 50-100 Km, depending on the location, from the eastern coast.

This general feature arisen from the tidal mixing involves the thermal fronts both at the surface and the bottom. The horizontal distributions of temperature at the surface and bottom may then indicate the location of these fronts. Fig. 1 shows the temperature distributions at 25m depth and the bottom, respectively. Since the fronts approach toward the center of the basin as one goes down (up) from the surface (bottom), this fact being observed in Fig. 2a for example, the surface front should occur nearer to the periphery of the basin than that at 25m depth. Also observed in Fig. 1 is the fact that fronts are stronger in the eastern half of the basin than the other. As mentioned earlier, this fact is compatible with the distribution of tidal energy dissipation obtained in Choi's (1980) numerical experiment. In subsequent analysis we therefore assume that the frontal structures induced by spatially different tidal action predominate in the Eastern Yellow Sea.

CIRCULATION

Fronts induced by tidal mixing are well explained by Van Heijst (1986) using the geostrophic adjustment model. In this model, the well mixed and stratified waters are initially separated by a vertical barrier. When this barrier is removed, the unstable density structure soon adjusts itself to geostrophic balance while retaining its initial vorticity. In final state, the induced currents and frontal shape

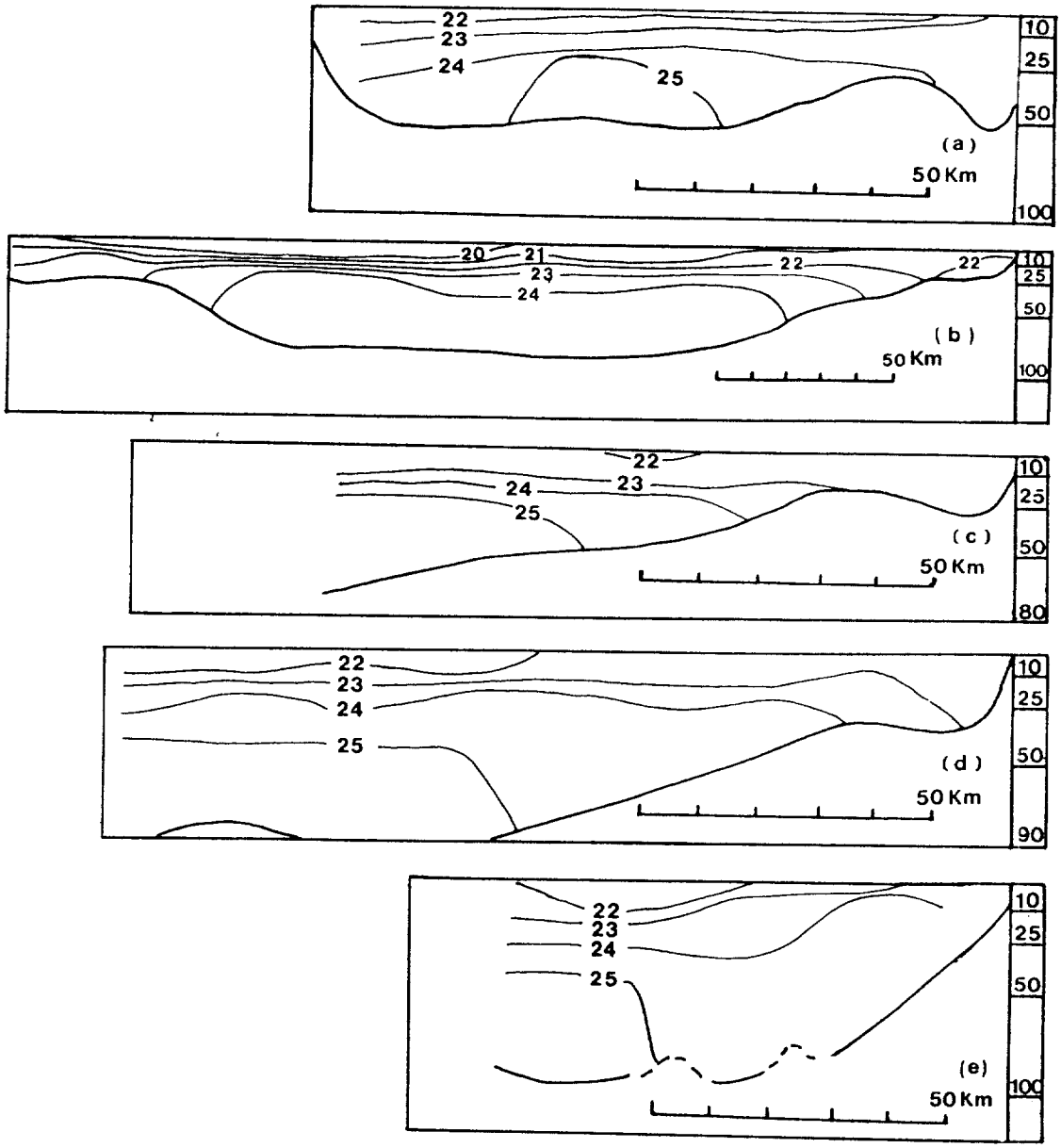

Fig. 3. Density structures on the sections a) L1, b) L3, c) L4, d) L5 and e) L6 (see Fig. 1 for locations). The section L3 is obtained in August, 1939 and others, in July, 1937 by Fisheries Experiment Station. Other expressions are in the same way as those in Fig. 2.

are in geostrophic balance.

To apply this model to study area, we therefore assume that the tidal mixing is complete in coastal area, and no tidal mixing at all in offshore area. These two areas are separated each other by a vertical barrier located some distance offshore from the coast and running parallel to the coastline. The area of interest is the eastern half of the basin because the frontal structure seems to be clearer here than the other as discussed above. In Fig. 2a and b for example, this corresponds

to the right half of the section.

This problem is therefore schematized in Fig. 4 for the case of two-layer ocean. The vertical barrier is located at $x = 0$ with mixed coastal water on the right ($x > 0$) and stratified offshore water on the left ($x < 0$). The frontal shapes in both initial and final (hypothetical) states are depicted in Fig. 4. Since the problem is non-linear, solutions are obtained for a particular set of parameters. However, the problem can be analytically tractable by assuming that the density interface between upper (density ρ_1) and lower (density ρ_3) layers remain horizontal during the adjustment process i.e., no vertical motion is induced at the interface. This assumption may be justified as follows: In non-dimensionalized adjustment problem like one considered here, the upper-to-lower layer depth ratio and the relative value of density difference determine the solution. Consider the case where the mixed layer water is pure mixture of local upper and lower layer waters. The density difference will then determine only the scale of front width as seen later in this paper. If the depth ratio is 1.0, the system becomes symmetric about the plane of mid-depth and the interface remains horizontal after ajustment. For depth ratio of 1/3 considered by van Heijst (1986, Fig. 4), the rise of interface after adjustment and its effect on the induced velocities are insignificant. In our case, the depth ratio is about 2/5 (cf., Fig. 2a and b for example), which lies between 1.0 and 1/3, and the interface is expected to remain nearly horizontal after adjustment. Under this assumption, therefore, the flow regime can be separated into two surface-to-bottom fronts; in other words, the surface $z = H_3$ in Fig. 4 can be considered as a rigid lid. The problem of surface-to-bottom front has already been solved analytically by Csanady (1978) and Stommel and Veronis (1980), and presented in Appendix.

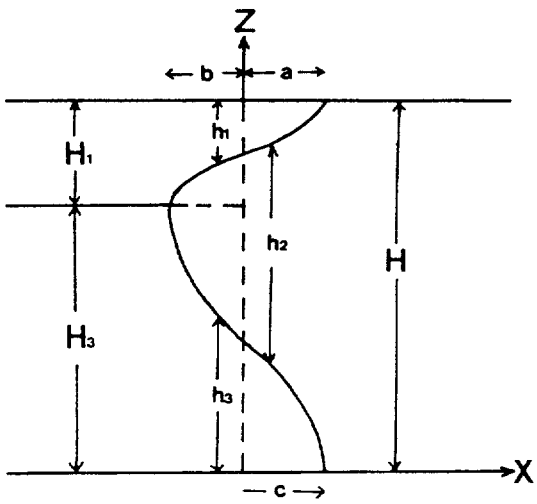

Fig. 4. Definition sketch of the model ocean. Dotted lines represent the initial state; and solid lines, final state. H and h mean the initial and final layer depths respectively. Subscripts 1 and 3 denote the upper and lower layers respectively. a,b and c are frontal distances.

In considering the upper ($z > H_3$) and lower ($z < H_3$) halves separately, a situation may happen that the fronts lying on both (up-and down-) sides of the plane $z = H_3$ occur at different horizontal positions. As shown below, this difficulty is removed in our case. In each of upper ($z > H_3$)and lower ($z < H_3$) halves, the radius of deformation R_o (cf., Appendix) is given by

$$R_o^u = \sqrt{g(\rho_2 - \rho_1) H_1/2\bar{\rho}}/f$$

$$R_o^l = \sqrt{g(\rho_3 - \rho_2) H_3/2\bar{\rho}}/f$$

where superscrips u and 1 represent the upper and lower halves respectively; g, the gravity constant; ρ_2, density of the mixed layer; $\bar{\rho}$, the mean density; H_1, depth of the upper half; H_3, depth of the lower half; and f, the Coriolis' parameter. Since ρ_2 is given by

$$\rho_2 = (H_1\rho_1 + H_3\rho_3)/(H_1 + H_3)$$

both R_o^u and R_o^l become equal to

$$R = \sqrt{g(\rho_3 - \rho_1) H_1H_3/2\bar{\rho}(H_1 + H_3)}/f$$

In a surface-to-bottom front problem, both the surface and bottom fronts occur at the

same distance from the vertical barrier: 1.2 times the radius of deformation (cf., Appendix). Since the radius of deformation in upper and lower halves are shown above to be the same each other, the frontal distances (a,b, and c in Fig. 4) then become equal to 1.2R. The difficulty arisen above is now resolved.

Solutions for layer depths (h_1, h_2 and h_3 for upper, mixed and lower layers, respectively) and northward (positive into the page) velocities (V_1,V_2 and V_3 with subscripts used in the same manner) are obtained by directly applying the results presented in Appendix:

$$h_i = \frac{H_i}{2}\left[1 - \frac{\sinh(x/R)}{\sinh(1.2)}\right] \quad (1)$$

$$V_i = -\frac{fR}{2}\left[\frac{x}{R} + \frac{\cosh(x/R)}{\sinh(1.2)}\right] \quad i = 1, 3 \quad (2)$$

$$h_2 = h_2^u + h_2^l = \frac{H}{2}\left[1 + \frac{\sinh(x/R)}{\sinh(1.2)}\right] \quad (3)$$

$$V_2 = -\frac{fR}{2}\left[\frac{x}{R} - \frac{\cosh(x/R)}{\sinh(1.2)}\right] \quad (4)$$

where h_2^u and h_2^l are solutions of h_2 obtained independently in upper and lower halves and $H = H_1 + H_3$ is the total water depth.

The resulting frontal shape is nearly the same as depicted in Fig. 4 except that $a = b = c = 1.2R$. This can be compared with the observation shown in Fig. 2a and b and Fig. 3a through e. For typical values of $g = 10 m/sec^2$, $\rho_3 - \rho_1 = 4.0 Kg/m^3$, $H_1 = 20m$, $H_3 = 50m$, $\bar{\rho} = 1.02 \times 10^3$ Kg/m^3 and $f = 10^{-4}/sec$, the radius of deformation becomes $R = 5.3$ Km and therefore the front width becomes $a + b = 12.8$ Km. The front width seems to be smaller than the observations shown in Fig. 2 and 3. This fact was already expected because the model idealizes the density structure by allowing a jump in tidal mixing. In reality, tidal mixing effect changes more gradually over the distance comparable with the basin width. In this context, the model-predicted transport, rather than the velocity, may have sense because the induced flows are overconcentrated within the narrow front width. Total transports are obtained from Eqs. (1) through (4) by using the typical values of parameters presented earlier. The mixed coastal water is transported northward by an amount of $2.95 \times 10^4 m^3/sec$; the surface water, $8.43 \times 10^3 m^3/sec$ in the opposite direction; the lower layer water (YSBCW), $2.11 \times 10^4 m^3/sec$ in the same direction as the surface water. However the sum of these transports vanishes. The obtained velocities are presented in Fig. 5, in which velocities are normalized by fR; and x, by R. For typical values of parameter given above, current speeds are up to about 0.64 m/sec with maximum at fronts. However, these speeds should be reduced by the same factor as that by which the real front width is larger than the model-predicted one. This fact is based on the arguments made earlier.

Due to the shallowness of the area, dynamic computation method such as done by Nakao (1977) may not be valid here for estimation of circulation. Numerical experiment performed by Choi (1982) for uniform southerly wind imposed over the whole basin shows a general circulation pattern of northward

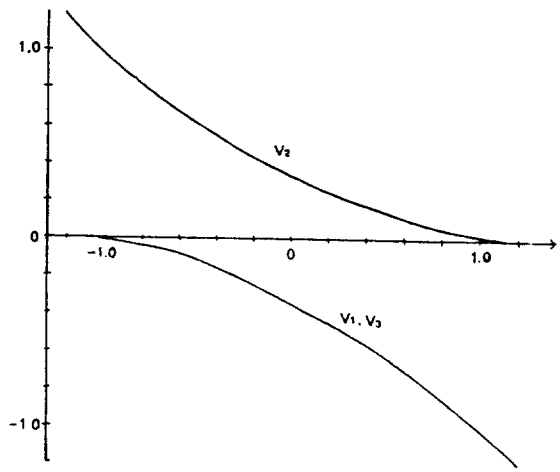

Fig. 5. Model-predicted velocites (V) as a function of horizontal distance (x). V and x are normalized by fR and R respectively. Subscripts 1 through 3 represent upper, mixed (coastal) and lower layers, respectively.

flows along the coastline and southward flow in central area. Though this experiment shows the circulation pattern somewhat similar to that obtained in this paper, the dynamic point of view is completely different: In his study, current is driven by wind imposed over the homogeneous water. His experiment thus may not reflect the reality in two respects: First, the effect of strong stratification is neglected and second, the real wind is not so persistently strong enough in summer.

CONCLUDING REMARKS

The density (temperature) structures in the Eastern Yellow Sea show a general feature that the tidal mixing fronts predominate in this area along the Korean coast. Application of geostrophic adjustment model gives a circulation pattern such that the mixed coastal water flows northward and the offshore waters (both surface warm and bottom cold) flow southward. The transport of each water amounts to $O(10^4)m^3/sec$. This model does not consider any smaller scale effects such as turbulent mixing by wind. This model also does not consider any barotropic component of current, such as induced by tidal effect and wind; though this component is not believed to be strong, the verification of this assumption is needed for completeness. For further extensive study on this area, more data are required. In this regard, it is most unfortunate that there is no sufficient measurement of current in this area and verification of the results, both obtained here and by others, still remain as another task.

ACKNOWLEDGEMENTS

The author thanks to C.H. Cho, S.Y. Nam and Y.S. Kang, the graduate students, for their help in drawing figures and typing text. Comments from referees are also acknowledged.

APPENDIX

In case where lighter water occupies the leftside of the initial barrier located at x = 0 (Fig. A), solutions for layer depth h and velocity V are given by

$$h_l = \frac{H_o}{2}\left[1 - \frac{\sinh(x/R)}{\sinh(d/R)}\right]$$

$$h_r = \frac{H_o}{2}\left[1 + \frac{\sinh(x/R)}{\sinh(d/R)}\right]$$

$$V_l = -\frac{fR}{2}\left[\frac{x}{R} + \frac{\cosh(x/R)}{\sinh(d/R)}\right]$$

$$V_r = -\frac{fR}{2}\left[\frac{x}{R} - \frac{\cosh(x/R)}{\sinh(d/R)}\right]$$

where the subscripts r and l refer to rightside (heavier) and leftside (lighter) waters respectively; $R = \sqrt{g'H_o}/2\ f$, the radius of deformation; $g' = g\ (Pr\text{-}\rho_l)/\bar{\rho}$, the reduced gravity; ρ, the density with $\bar{\rho}$ denoting its mean value; g, the gravity; f, the Coriolis' parameter; H_o, the water depth; and d = 1.2R, the distance of both surface and bottom fronts measured from x = 0. In case where heavier water initially lies on the leftside of the barrier, and conversely for lighter water, the resulting

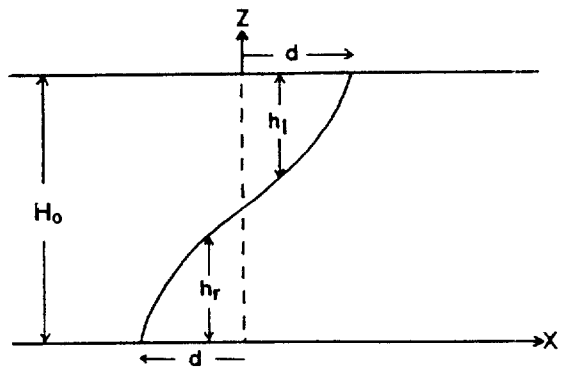

Fig. A. Definition sketch of model ocean for surface-to-bottom front problem. Dotted line represents the initial state; and solid line, the final state. h is the final layer depth and H_O is the total depth. Subscripts l and r denote the intial location of two waters, namely, leftside (l) and rightside (r) of the barrier. d is the frontal distance. Leftside water is lighter than the rightside water.

frontal shape becomes reversed about the mid-depth $z = H_o/2$ and all expressions for h and V are interchanged between the two waters.

REFERENCES

Choi, B.H., 1980. A tidal model of the Yellow Sea and the Eastern China Sea. KORDI Rep. 80-02, BSPI 00019 (3)-36-2,72pp.

Choi, B.H., 1982. Note on currents driven by a steady uniform wind system on the Yellow Sea and the East China Sea. La Mer, **20**: 65-74.

Csanady, G.T., 1978. Wind effects on surface-to-bottom fronts. J. Geophys. Res., **83**: 4633-4640.

KORDI, 1986. A study on the Atlas of Marine Resources in the Adjacent Seas to Korea-Yellow Sea: spring, fall, and winter seasons. KORDI Rep., BSPG 00030-119-7,523pp.

Lie, H.J., 1984. A note on water masses and general circulation in the Yellow Sea (Hwang Hae). J. Oceanol. Soc. Korea, **19**: 187-194.

Nakao, T., 1977. Oceanic variability in relation to fisheries in the East China Sea and the Yellow Sea. J. Fac. Mar. Sci. Tech., Tokai Univ., Spec. No.: 199-367.

Stommel, H. and G. Veronis., 1980. Barotropic response to cooling. J. Geophys. Res., **85**: 6661-6666.

Van Heijst, G.J.F., 1986. A geostrophic adjustment model of tidal mixing front. J. Phys. Oceanogr., **15**: 1182-1190.

Received February 16, 1987
Accepted April 15, 1987